Experimental Neurology 311 (2019) 162–172

Contents lists available at ScienceDirect

Experimental Neurology

journal homepage: www.elsevier.com/locate/yexnr

Research Paper

Insulin-like Growth Factor (IGF)-1 treatment stabilizes the microvascular cytoskeleton under ischemic conditions

Shameena Bake[a,1], Andre Okoreeh[a,1], Homa Khosravian[b], Farida Sohrabji[a,*]

[a] Women's Health in Neuroscience Program, Neuroscience and Experimental Therapeutics, Texas A&M College of Medicine, Bryan, TX 77807, United States
[b] Department of Chemical Engineering, Texas A&M University, College Station, TX 77840, United States

ARTICLE INFO

Keywords:
Blood brain barrier
Cerebral ischemia
Brain microvascular endothelial cells
Vinculin
Oxygen-glucose deprivation
Intercellular spaces

ABSTRACT

Our previous studies showed that Insulin-like Growth Factor (IGF)-1 reduced blood brain barrier permeability and decreased infarct volume caused by middle cerebral artery occlusion (MCAo) in middle aged female rats. Similarly, cultures of primary brain microvessel endothelial cells from middle-aged female rats and exposed to stroke-like conditions (oxygen glucose deprivation; OGD) confirmed that IGF-1 reduced dye transfer across this cell monolayer. Surprisingly, IGF-1 did not attenuate endothelial cell death caused by OGD. To reconcile these findings, the present study tested the hypothesis that, at the earliest phase of ischemia, IGF-1 promotes barrier function by increasing anchorage and stabilizing cell geometry of surviving endothelial cells. Cultures of human brain microvessel endothelial cells were subject to oxygen-glucose deprivation (OGD) in the presence of IGF-1, IGF-1 + JB-1 (IGFR inhibitor) or vehicle. OGD disrupted the cell monolayer and reduced cell-cell interactions, which was preserved in IGF-1-treated cultures and reversed by concurrent treatment with JB-1. IGF-1-mediated preservation of the endothelial monolayer was reversed with LY294002 treatment, but not by Rapamycin, indicating that IGF-1 s actions on cell-cell contacts are likely mediated via the PI3K pathway. In vivo, microvessel morphology was evaluated in middle-aged female rats that were subjected to ischemia by MCAo, and treated ICV with IGF—I, IGF-1 + JB-1, or artificial CSF (aCSF; vehicle) after reperfusion. Compared to vehicle controls, IGF-1 treated animals displayed larger microvessel diameters in the peri-infarct area and increased staining density for vinculin, an anchorage protein. Both these measures were reversed by concurrent IGF-1 + JB-1 treatment. Moreover these effects were restricted to 24 h after ischemia-reperfusion and no treatment effects were seen at 5d post stroke. Collectively, these data suggest that in the earliest hours during ischemia, IGF-1 promotes receptor-mediated anchorage of endothelial cells, and its actions may be accurately characterized as vasculoprotective.

1. Introduction

Ischemic stroke causes loss of nutrients to brain tissue and initiates a sequence of harmful events within neurons including rapid failure of ATP-dependent processes, increased release of glutamate and calcium, and rapid cell death (Pulsinelli, 1992; Moskowitz et al., 2010; Khatri et al., 2012). The earliest impact of ischemia includes changes in the blood brain barrier, followed by vasogenic edema in the brain (Yang et al., 2007). These deleterious changes to the barrier are accompanied by disruption of intercellular tight junction assembly causing microvessel hyperpermeability (Kreuger and Phillipson, 2016), heightened inflammatory responses (Gidday et al., 2005; Kleinschnitz and Wiendl, 2013) and loss of anchorage of endothelial cells (Baldo et al., 2015). Cell surface alterations on the endothelium such as the upregulation of adhesion molecules ICAM-1 and CCL2 facilitates infiltration of neutrophils and macrophages into the brain during the early phase of injury (Dimitrijevic et al., 2007; Wu et al., 2015; Shi et al., 2016; Zhu et al., 2016). Blood brain barrier hyperpermeability and edema is associated with poor prognosis (Khatri et al., 2012), and consistent with this observation, stroke-induced brain damage and disability and blood-brain barrier permeability is significantly higher in older animals as compared to young animals (Dinapoli et al., 2008; Liu et al., 2009; Montagne et al., 2015). Hence, the blood brain barrier and its component cells are critical for stroke pathophysiology and are considered important targets for stroke therapy (Borlongan et al., 2012; Merali et al., 2016)

* Corresponding author at: Neuroscience and Experimental Therapeutics, Texas A&M College of Medicine, MREB 4102 State Hwy 47, Bryan, TX 77807, United States.
E-mail address: Sohrabji@medicine.tamhsc.edu (F. Sohrabji).
[1] equal contributors.

https://doi.org/10.1016/j.expneurol.2018.09.016
Received 23 July 2018; Received in revised form 29 August 2018; Accepted 27 September 2018
Available online 01 October 2018
0014-4886/

Our previous studies show that middle-aged female rats sustain larger infarcts and worse stroke outcomes as compared to younger females (Selvamani and Sohrabji, 2010a,b), and this is associated with decreased levels of circulating and parenchymal IGF-1. Accordingly, intracerebroventricular (ICV) delivery of IGF-1 2 h after ischemia to middle-aged female rats reduces infarct volume when measured 24 h after stroke. In silico analysis of epigenetic modulators indicated that IGF-1 regulated microRNAs that improve extracellular matrix interactions and endothelial cells. We focused on blood brain barrier changes and reported that as early as 4 h after MCAo, IGF-1 treatment decreased blood brain barrier permeability to small molecules (Bake et al., 2014) although the peptide did not reduce infarct volume at this time point. At 48 h after MCAo, when brain trafficking of T-regulatory cells was seen, IGF-1 reduced passage of these larger elements as well (Bake et al., 2014; Bake et al., 2016). Ex vivo cultures of primary brain microvascular endothelial cells (BMECs) from middle-aged rats subject to OGD showed that IGF-1 reduced transfer of FITC-BSA transfer across the monolayer (Bake et al., 2016), but did not prevent cell death. These data suggest that IGF-1 actions during the earliest phase of ischemia are not dependent on cell survival, but may act via a different mechanism. The present study employed complementary in vivo and in vitro approaches to test whether IGF-1 prevents ischemia-induced cytoskeletal rearrangement and cell detachment from the extracellular matrix.

2. Materials and methods

2.1. In vitro studies

2.1.1. Cell culture and oxygen glucose deprivation (OGD)

Human brain microvascular endothelial cells (hBMEC) were purchased from Millipore Corp. MA (hCMEC/D3,) and grown with EndoGro medium (Millipore Corp. MA) on type I collagen-coated T-75 flasks. For experiments, cells (5×10^4) were plated either on collagen-coated coverslips or in 96-well plates and maintained until confluent. Cultures were grown in normoxic conditions (5% CO2 and 21% O2; 37 °C) until confluent. Cells were then subject to OGD (1% O2, 95% N2 and 5% CO2 in glucose free DMEM) for 6 h with IGF-1 (10 ng/ml), IGF-1 + JB-1 (IGF-1 receptor antagonist; 2 ng/ml), IGF1 + LY294002 (reversible PI3-kinase inhibitor, 1 μg/ml) and rapamycin (mTOR inhibitor, 1μg/ml) or vehicle (PBS or DMSO). Culture media was collected for assays and cells were fixed for histological analysis. All assays were conducted with 3–5 replicate runs and each run consisted of 5–6 technical replicates.

2.1.2. Quantitative (q)RT-PCR

Human IGF1R mRNA expression in hBMEC was assessed using real-time qRT-PCR. Total RNA was extracted using QIAzol reagent and RNA Mini extraction kit (Qiagen, CA) using our previous procedures (Okoreeh et al., 2017). RNA yield and purity were evaluated with a NanoDrop ND-1000 spectrophotometer (NanoDrop Technologies/ Thermo Scientific). 100 ng of purified total RNA was used to generate cDNA, using a cDNA Synthesis Kit (Quantbio, MA) following manufacturer's protocol. cDNA was diluted 80 fold and real time PCR reaction were run on Applied Biosystems 7900HT real-time PCR instrument (Applied Biosystems, CA) using a SYBR green-based real-time PCR reaction kit (Quantabio, MA). 18 s mRNA was used as a normalization control. Human IGF-1R (Forward:5′- TTA AGA ACC AGT GGC GAA AG -3′, Reverse: 5′- GGA GCA CTC ACT TCT CCA AA -3′ Realtime primers, PA) and 18S primers (Forward:%'-ATGGCCGTTCTTAGTTGGTG -3′; Reverse: 5′-CGCTGAGCCAGTCAGTGTAG-3′, Life Technologies, CA).

2.1.3. Cell death/survival assays

2.1.3.1. LDH assay. Cell death was estimated by lactate dehydrogenase (LDH) in media immediately after collection, using a colorimetric assay (Thermofisher, MA) and our previous procedures (Bake et al., 2016). Briefly, 50 μl of culture media was added to each well of a 96-well plate and mixed with catalyst and dye substrate mixture. After incubation for 30 min, 50 μl of stop solution was added to each well and the plate was read at 490 nm absorbance on a colorometric plate reader (Tecan, Switzerland). **Calcein assay:** Cell viability was determined using the Calcein-AM dye (Life Technologies,CA). After OGD, cells were incubated with calcein-AM (2.5 μm) in PBS for 20 min at 37 °C and the fluorescence was measured on a plate reader (Tecan, Switzerland) with excitation/ emission set at 480 and 530 nm respectively.

2.1.3.2. Phalloidin staining. Endothelial cells grown on coverslips were washed and fixed with 4% paraformaldehyde, and then permeabilized in 0.1% triton-X and washed three times with PBS. Cells were then incubated with 3% BSA for 20 min followed by two washes and stained with Alexa Fluor 488 phalloidin (Life technologies, CA) for 30 min, washed with PBS and mounted with Prolong antifade mounting media (Life technologies, CA). Images were captured on the FSX100 Olympus microscope.

2.1.3.3. Vinculin immunohistochemistry. Endothelial cells grown on coverslips were processed for immunohistochemistry using our previously published procedures (Bake et al., 2016). Briefly, cells were incubated in a blocking solution (2% normal goat serum and 2% triton X-100 in dPBS) for 1 h at room temperature, followed by incubation with the antibody for vinculin (eBioscience, San Diego, CA, 1:100) overnight. Following 3 PBS washes, cells were then incubated for 1 h with fluorescent-labeled secondary antibody (Alexa Fluor 594 goat anti-mouse, 1:500 dilution) and were counterstained with nuclear dye (Hoechst, 1:500) and coverslipped with Prolong antifade mounting media (Life technologies, CA). Images were captured using an Olympus confocal microscope.

2.1.3.4. Lectin staining. In vitro analysis: Endothelial cells grown on coverslips were washed and fixed with 4% paraformaldehyde, and then permeabilized in 0.1% triton-X and washed three times with PBS. Cells were then incubated with 3% BSA for 20 min followed by two washes and stained with lectin (1:1000, Vector Laboratories, CA) for 30 min, washed with PBS and mounted with Prolong antifade mounting media. Images were captured on the FSX100 Olympus microscope. *Determination of intercellular spaces*: Lectin-stained cell cultures (3 experimental replicates) were photographed, coded and analyzed for continuity of the monolayer using a novel algorithm to determine intercellular 'spaces'. Briefly, all images were first converted into grayscale images. A threshold was calibrated for each image to convert the grayscale image into a black and white one, such that cells are in white and everything else remains black. Thus, the total number of gaps between cells in each image was estimated by the total number of black pixels. Once the cells were identified, the two images were overlaid to find all the cells and the near empty areas in the image. The spaces near cells were calculated using the Canny edge detection algorithm. The above algorithm was coded in Python and OpenCV.

2.2. In vivo studies

2.2.1. Animals

Female Sprague Dawley (SD) rats were purchased as retired breeders (10–12 months; weight range 325–350 g) from Envigo Laboratories (previously Harlan Labs, IN). This group met our previously established criteria for reproductive senescence, namely, at least five successful pregnancies and current acyclicity determined by daily vaginal smears. All animals were housed in an AAALAC–approved facility, maintained on a constant photoperiod (12-h light/dark cycles), and fed ad libitum with laboratory chow (Harlan Teklad 8604) and water. All animal procedures were performed in accordance with the National Institutes of Health guidelines for the humane care of laboratory animals and were approved by the Institutional Animal Care Committee and the Institutional Biosafety Committee. A total of 55 animals were used in

this study, with 7–9 animals per group for behavioral analysis and 5–6 animals per group for histological analysis.

3. Surgical procedures

3.1. Cannula implantation

Animals were placed in a stereotaxic instrument (David Kopf instruments, CA), a 28 gauge cannula was implanted into the right lateral ventricle using the co-ordinates – 1.0 mm posterior to bregma, −1.4 mm medial lateral, −3.5 mm from dural surface, and anchored in place with loctite 454 (Braintree Scientific, MA). Animals were allowed to recover for 1 week following cannula implantation and prior to stroke surgery. Alzet osmotic minipumps (1003D & 1007D, Alzet corp., CA, flow rate 0.5 and 1 μl/h) filled with human recombinant (rh)IGF-1 (R&D Laboratories, 100 μg/ml) or rhIGF-1 and JB-1 (20 μg/ml) were primed overnight and placed into a subcutaneous pocket between the scapula and spine, after 45 min of ischemia. IGF-1 delivery to the brain initiated 2 h after the onset of ischemia. Previous studies have shown that IGF-1 is stable in Alzet minipumps for up to 7 days. Control animals were infused with artificial CSF. All animals were terminated either 1 day or 5 days post-reperfusion.

3.2. Middle cerebral artery occlusion (MCAo)

Animals were subjected to middle cerebral artery occlusion (MCAo) via intraluminal suture 1 week after cannula implantation, using our previous procedures (Bake et al., 2014; Bake et al., 2016). Briefly, rats were anesthetized with isoflurane and maintained at 37 °C on heating pads in dorsal recumbency. The neck region was shaved and disinfected and a ventral midline incision was made on the skin. Superficial fascia on the right side of the neck was dissected and the underlying muscles were blunt dissected to expose the right common carotid (CCA), external (ECA), and internal carotid (ICA) arteries. The ECA was separated from the vagus nerve and tied off distally with silk sutures after cauterizing the small branches. Microsurgical clamps were placed on CCA and ICA. A loose tie was placed on the ECA, and the free stump of ECA was aligned with the ICA. 22 mm of suture of the appropriate size (37–41) with a silicon-coated round tip (Doccol Corp., CA) was inserted into ICA lumen through a small nick on the ECA between the two ties. The suture was advanced along the ICA until it reached the origin of the MCA (~20 mm of suture) and secured in position with nylon ties. The intraluminal suture was maintained for 90 min and then withdrawn. Tissue perfusion rate was monitored using Laser-Doppler Flowmetry (Moor Instruments, UK) and the perfusion index was calculated for both ischemic and reperfusion time points. MCAo resulted in an 80% reduction of blood flow compared to the pre-occlusion rate and re-perfusion restored the perfusion index back to pre-occlusion levels. All animals were carefully monitored after surgery and terminated 1 day or 5 days after ischemia.

4. Behavioral analysis

4.1. Neurological score

Functional tests were performed 1 day after MCAo. Each animal underwent five tests in succession to assess motility, grasping, righting reflex, forepaw disability, and circling, as described in (Bake et al., 2016; Okoreeh et al., 2017). For each test, a higher score indicates a more severe deficit.

4.2. Histological analyses

Animals were deeply anesthetized with ketamine/xylazine (ketamine: 87 mg/kg; xylazine: 13 mg/kg) and then perfused transcardially with saline followed by a perfusion fix solution (4% paraformaldehyde, 4% sucrose in dPBS) and decapitated. Heads were placed in a container filled with perfusion fix solution overnight at room temperature. Subsequently, the brains were removed from the cranial vault and stored in Dulbecco's phosphate saline with 0.01% sodium azide until shipped to Neuroscience Associates (NSA, Nashville, TN) for processing. Briefly, brains were block embedded in MultiBrain® blocks and freeze-sectioned at 40 μm with a sliding microtome, yielding free-floating sections collected in antigen preservation solution.

4.2.1. Vinculin immunohistochemistry

Brain sections (40 μm) containing cortex and striatum were mounted and adhered to gelatin-coated glass slides and processed for vinculin immunohistochemistry as described above and analyzed as follows. Three images were captured from the peri-infarct zone of the cortex and striatum of the immunostained section for each animal, using a Q-color camera attached to the FSX100 Olympus microscope. The section was at the interaural level 8.7 mm, bregma −0.30 mm (Paxinos and Watson, 1986). Photomicrographs were coded and then analyzed for vinculin staining density using ImageJ software (NIH, MD). In each image, three regions were demarcated and the area occupied by vinculin particles were measured in each region. The area occupied by vinculin particles was then normalized to the area of the box to obtain the density of vinculin label. For each animal, density measurements were obtained separately for the cortex and striatum and then combined to obtain a single value for each animal. Both the ischemic and non-ischemic hemispheres were analyzed. Data was decoded and analyzed by 2 way ANOVA coded for hemisphere (repeated measure) and treatment condition. Separate analyses were performed for day 1 and day 5 post stroke (SPSS, IBM).

4.2.2. Lectin

Brain sections (40 μm) were mounted and adhered to gelatin-coated glass slides and stained for lectin as described above. Lectin-stained vessels were analyzed in the following way. Three images were captured each from the cortex and striatum of the immunostained section for each animal, using a Q-color camera attached to the FSX100 Olympus microscope. The section was at the interaural level 8.7 mm, bregma −0.30 mm (Paxinos and Watson, 1986). Images were coded and processed in Autoquant X3 (Mediacybernetics,US) and were analyzed for diameter and length of microvessels with Imaris (Bitplane, US). For each animal, values were obtained separately for the cortex and striatum and then combined and binned into 3 groups, 1-5 um, 6–10 um, 11 + um. Data was decoded and analyzed by 2 way ANOVA coded for treatment condition and bin (repeated measure). Due to the volume of data and the possibility of spurious errors, separate analyses were performed for each hemisphere and for day 1 and day 5 post stroke (SPSS, IBM).

4.2.3. Statistical analysis

Group differences were analyzed using SPSS Statistic 23 software (IBM) and differences were considered significant at $p < 0.05$. For in vitro studies, 3 to 4 biological replicates were prepared with 6 technical replicates per run. Each run was normalized to its normoxic control group and one way ANOVA was used to evaluate group differences, with planned comparisons. For in vivo studies, neurological scores were analyzed by one way ANOVA. Vinculin and lectin histology was analyzed as described above. Data are expressed as mean ± SEM.

5. Results

5.1. IGF-1 does not reduce OGD-induced cell death

Media LDH from normoxic cultures and cultures exposed to OGD, with various treatments, was used as a surrogate marker for cytotoxicity (Fig. 1A). Groups were compared using a one-way ANOVA with planned post hoc comparisons ($F_{(5,18)}$: 2.56, $p = 0.084$). Compared to

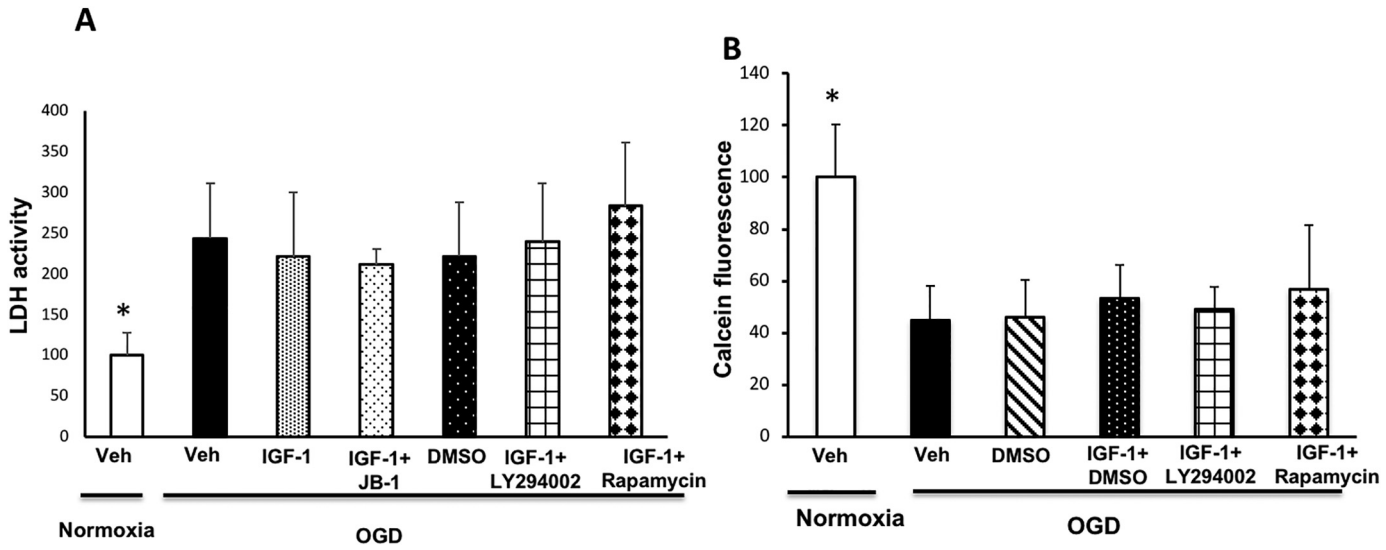

Fig. 1. Effect of IGF-1 on human brain microvascular endothelial cell (hBMECs) survival: A. LDH levels in the media from normoxic cultures were significantly lower than cultures exposed to OGD. IGF-1 treatment, with or without its receptor inhibitor (JB-1) or signaling pathway inhibitors had no effect on OGD-induced LDH levels. B. Calcein assay: Cell survival as measured by calcein was significantly lower in cultures exposed to OGD as compared to normoxic cultures. Here also, IGF-1 treatment, with or without signaling pathway inhibitors showed no significant difference in cell viability. Histograms depict mean and SEM. Each data point is the average of 6 technical replicates, and shown here is the average from 3 separate experiments. *$p < 0.05$, normoxia as compared to all other groups.

normoxia, LDH levels were significantly elevated by 6 h of OGD ($p = 0.045$). Neither IGF-1 ($p = 0.46$) nor concurrent IGF-1 + JB-1 ($p = 0.37$) reduced LDH release under OGD conditions. Similarly, LY294002 ($p = 0.94$) or Rapamycin ($p = 0.55$) also did not reduce OGD induced levels of LDH. In addition, cell survival was also determined by the calcein-AM assay (Fig. 1B), using a one way ANOVA and planned post hoc comparisons ($F(5,17):2.73$; $p = 0.077$). OGD significantly decreased cell survival as measured by calcein ($p = 0.017$). Here also IGF-1 treatment ($p = 0.67$), with and without Rapamycin ($p = 0.83$), or LY294002 ($p = 0.56$) did not improve cell survival. Collectively, these studies confirm that IGF-1 does not reduce cell death in the ongoing ischemic environment. Expression of IGF1R in hBMECs were confirmed with qRT-PCR and did not show any difference between normoxia and OGD (Supplementary Fig. 1).

5.2. IGF-1 preserved the actin cytoskeleton of human brain microvascular endothelial cells after OGD

To determine whether IGF-1 improved endothelial cytoskeletal organization and cell adherence under OGD, cells were probed for phalloidin (actin) and vinculin, a membrane-cytoskeletal protein associated with cell-cell and cell-matrix junctions. Normoxic cells displayed either round or flattened profiles, with actin staining (in green, Fig. 2B) localized to the edges of the cell (circular actin). While flattened cells displayed pale phalloidin staining, vinculin labeling (shown in red; Fig. 2A) was seen in the cytoplasm as well as at the cell perimeter. Oxygen-glucose deprivation (OGD) visibly decreased cell density and caused cytoskeletal reorganization of surviving cells. Thick, brightly stained stress fibers (in green) can be seen in cells that are elongated (Fig. 2C,) and with decreased vinculin staining. Under the same conditions, cells treated with IGF-1 showed flattened cell morphology with bright vinculin labeling in the cytoplasm and at the edges (Fig. 2E) with reduced density of polymerized actin across the cells (Fig. 2F). This pattern was reversed by concurrent treatment with JB-1. Cells treated concurrently with IGF-1 + JB-1 closely resembled the OGD treated cultures in the pattern of brightly stained stress fibers with more retraction of actin and diffuse vinculin labeling (Fig. 2G and H) indicating a receptor-mediated effect of IGF-1 on cytoskeletal reorganization.

To quantify the extent of OGD-dependent retraction of the endothelial cell monolayer, cultures were stained with lectin (Fig. 3Ai). Lectin staining further confirmed that oxygen glucose deprivation caused significant retraction of cells resulting in discontinuous aggregates of small groups of cells. This pattern was quantified using a novel algorithm that calculates intercellular (IC) spaces (Fig. 3Aii). This analysis showed an overall affect of OGD and IGF-1 on interceullar spaces ($F(3,12)$: 5.864, $p = 0.020$). Specifically, OGD increased intercellular spaces as compared to normoxia ($p = 0.017$), while IGF-1 treatment reduced cell shrinkage due to OGD, and was no different from normoxia ($p = 0.226$). IGF-1 effects were reversed in cultures concurrently exposed to IGF-1 + JB1 ($p = 0.004$, compared to normoxia). Quantitation of the intercellular gaps (Fig. 3Bii) also confirmed that IGF-1 signaling inhibitors had distinct effects on IC spaces ($F_{(5,12)}$: 4.99, $p = 0.01$). Thus while OGD and OGD (vehicle control or DMSO) caused a > 5 fold increase in intercellular spaces as compared to normoxic cultures ($p = 0.001$), this was reversed by. IGF1 ($p > 0.05$). The effect of IGF-1 on IC spaces was abrogated by concurrent treatment with LY294002 ($p = 0.020$ compared to normoxia), but not Rapamycin ($p = 0.277$) compared to normoxia), indicating that IGF-1 actions on the endothelial monolayer are mediated by PI3K but not the mTOR pathway.

5.3. Impact of IGF-1 on microvessel architecture in vivo

To determine if IGF-1 acts on microvessel anchorage and morphology in vivo, middle-aged female rats were subject to MCAo for 90 mins and treated with IGF-1 or IGF-1 + JB-1 or aCSF (vehicle) 2 h after the onset of ischemia. Neurological score, an assessment of motor function, was performed 24 h after reperfusion by an investigator (AO) blind to the treatment conditions. Vehicle-treated controls had a high mean score (4.28) indicative of greater disability, as compared to IGF-1-treated animals (2.5) ($p = 0.0477$) (Fig. 4). In contrast, animals that received concurrent IGF-1 + JB-1 performed as poorly (3.9), as the vehicle-treated controls ($p = 0.612$) and were significantly higher than animals which received IGF-1 only ($p = 0.016$), indicating that IGF-1 treatment protects motor function and mobility post-stroke in a receptor-mediated process.

5.4. Effect of post-stroke IGF-1 treatment on vinculin staining

Brain sections from animals subject to MCAo were probed for

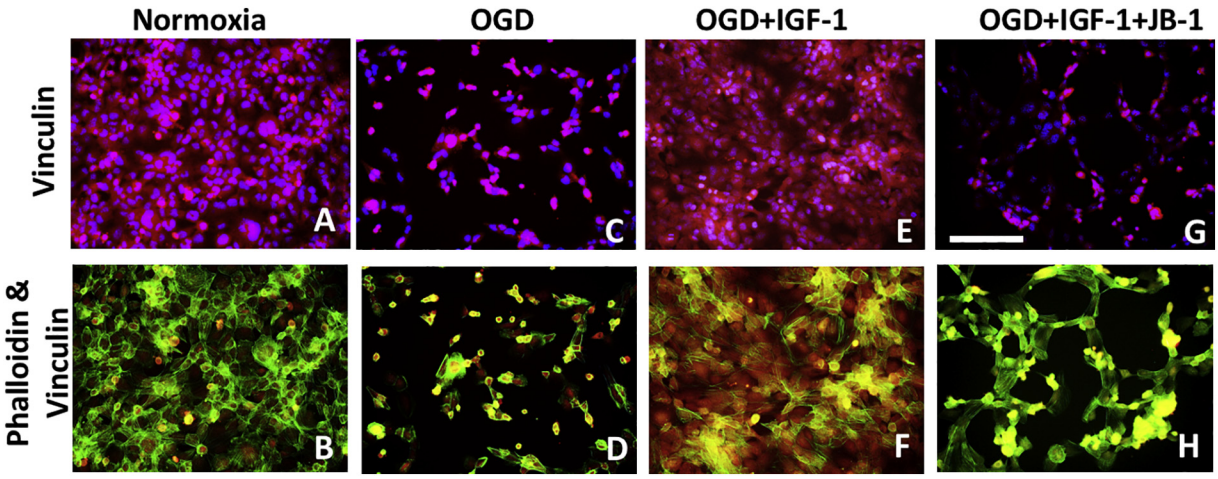

Fig. 2. Effect of IGF-1 on hBMECs cell adhesion and cytoskeletal organization: Compared to normoxic conditions (A and B), cultures exposed to OGD show retracted cells with low vinculin labeling (C) and bright stress fibers (green phalloidin, D). IGF-1-treated cells displayed flattened cell morphology, similar to normoxic conditions, with brighter vinculin staining both in the cytoplasm and at the cell perimeter (E), with fewer stress fibers compared to OGD (F), while this pattern was reversed in cells treated concurrently with IGF-1 + JB-1 (G&H). Bar: 50 um. (For interpretation of the references to color in this figure legend, the reader is referred to the web version of this article.)

vinculin immunohistochemistry. Striatal and overlying cortical regions were analyzed for density of vinculin labeling. Representative sections of each group at 1 day post stroke are shown in Fig. 5A. Punctate vinculin label was seen in the cortex and striatum of all experimental groups 24 h after ischemia-reperfusion (Fig. 5A), however, vinculin staining density was significantly higher in the IGF-1-treated group as compared to the vehicle-treated controls or to groups that received concurrent IGF-1 + JB-1 ($F_{(2,13)}$: 5.021; p = 0.028) (interaction effect). At 5-day post-stroke, there was no statistical difference in vinculin staining density between treatment groups (Fig. 5B).

5.5. Effect of post-stroke IGF-1 treatment on microvessel morphology

Sections from control, IGF-1 and IGF-1 + JB-1 treated groups subject to MCAo were stained for lectin histochemistry. Representative sections of each group at 1 day post-stroke is shown in Fig. 6A. A minimum of 50 vessels were analyzed per animal and grouped as small (1–5 μm) medium (6–10 μm) or large (11 + μm) diameter vessels. In the ischemic hemisphere, IGF-1-treated animals had a significantly greater proportion of large diameter vessels as compared to vehicle-treated controls or JB-1 treated animals ($F_{(2,11)}$ = 21.707; p < 0.001) and the lowest proportion of small diameter vessels ($F_{(2,11)}$ = 9.696; p = 0.004), indicating that IGF-1 treatment skews the distribution towards larger-diameter microvessels. A similar pattern was also seen in the non-ischemic hemisphere, where IGF-1 treated animals displayed the highest proportion of large diameter vessels ($F_{(2,12)}$ = 6.639; p < 0.011), and the lowest proportion of small diameter vessels ($1F_{(2,12)}$ = 8.752; p = 0.005) as compared to vehicle treated controls and JB-1 treated animals.

At 1 day post stroke, microvessel length was partly influenced by IGF-1 treatment. There was a significant decrease in the proportion of short length vessels ($F_{(2,11)}$ = 4.169; p < 0.042), and a trend towards longer length vessels ($F_{(2,12)}$ = 3.01; p < 0.087) in IGF-1 treated animals as compared to vehicle treated controls or JB-1 treated animals (Fig. 6A). On the non-ischemic hemisphere, there were no differences in vessel length between IGF-1 and vehicle treated controls.

At 5 days post stroke (Fig. 6B), all groups had a similar proportion (19%–20%) of large diameter vessels, while IGF-1 treated animals had more small diameter vessels and fewer medium diameter vessels as compared to vehicle treated controls or JB-1 treated animals. No treatment effects were noted for the non-ischemic hemisphere at 5d post stroke, although most microvessels fell in the medium and large diameter category unlike the ischemic side where most vessels fell in the medium and small diameter category, indicating an overall shift in vessel diameter due to ischemia.

There were no treatment effects on microvessel length at 5d after stroke, in either the ischemic or non-ischemic hemisphere (Fig. 6B). Moreover, both sides showed similar distributions in small, medium and large length vessels. Overall, IGF-1 exerted an early effect on vessel diameter.

6. Discussion

Our previous work showed that IGF-1 treatment to endothelial cell cultures protects the barrier properties of these cells under OGD conditions. We also reported that IGF-1 does not prevent cell death during OGD conditions, which seems paradoxical in light of IGF-1's effects on barrier function. The current studies provide an answer to this paradox, by showing that while OGD conditions cause endothelial cells shrinkage (and therefore prominent intercellular spaces), IGF-1 treatment preserves the flattened morphology and anchorage of surviving cells (fewer intercellular spaces), thus potentially maintaining a more effective barrier. In view of the short duration of OGD (6 h), it is unlikely that the reduced intercellular space is due to cell proliferation, and likely represents IGF-1 action on the actin cytoskeleton of surviving cells. In vivo, microvessel diameter, a surrogate measure of cell contraction (Shen et al., 2009) showed that IGF-1 treated animals had larger microvessel diameter in the ischemic region at 24 h after stroke and greater density of vinculin staining, further supporting the idea that IGF-1 stabilizes the endothelium. Together with our previous in vivo studies showing that IGF-1 treatment to middle-aged female rats decreases BBB permeability (Bake et al., 2014) and infiltration of CD4 + cells into the ischemic brain (Bake et al., 2016), the current studies show that IGF-1 is a vasculoprotective factor in stroke.

IGF-1 is considered neuroprotective because it reduces ischemic injury in many species (Gluckman et al., 1992; Lee et al., 1992; Johnston et al., 1996; Guan et al., 2001) and promotes neuronal survival, neuronal myelination and angiogenesis (Wang et al., 2000; Smith, 2003). However, vascular pathology is among the earliest events in ischemic stroke. During the acute phase after reperfusion, accumulation of toxic oxygen radicals impair endothelial function leading to a leaky blood brain barrier. In the hours following stroke (sub-acute phase), barrier permeability is increased due to the generation of inflammatory cytokines, endothelial adhesion molecules and proteinases

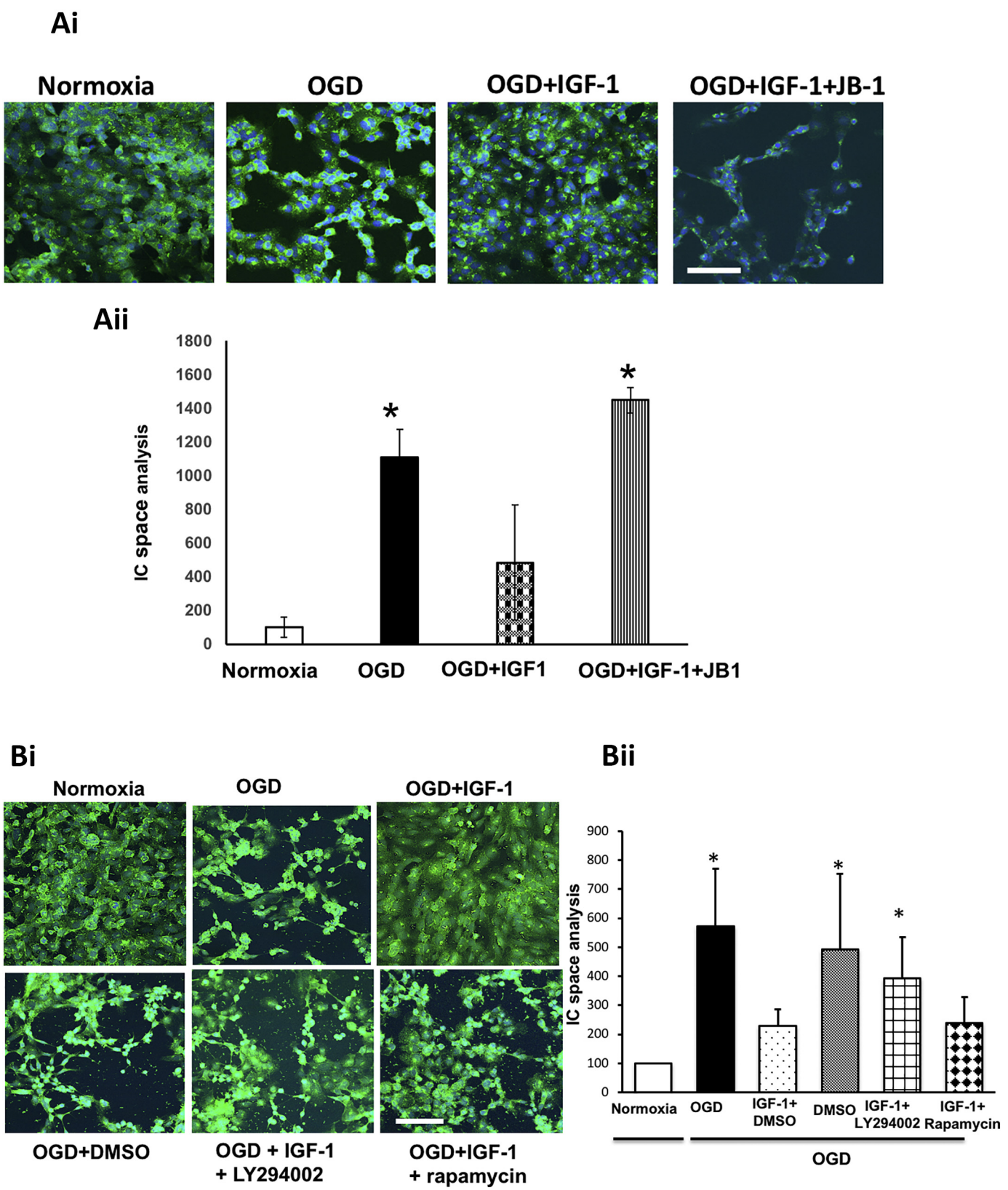

Fig. 3. Lectin staining of human brain microvessel endothelial cells (hBMEC) under normoxic and OGD conditions. Ai. Effect of IGF-1 and its receptor antagonist on intercellular spaces: Photomicrographs of lectin-stained cultures show that the even, confluent monolayer seen in normoxia is changed under OGD to smaller, densely-stained cells with large intercellular spaces. Intercellular spaces were completely abrogated in IGF-1 treated cultures and this was reversed with concurrent exposure to JB-1. Aii Histogram shows average intercellular space estimates using the Canny Edge algorithm. B ii. Effect of IGF-1 and signaling pathway inhibitors on intercellular spaces: Photomicrographs of lectin-stained cultures confirm that IGF-1 abrogates intercellular spaces caused by OGD. All experimental groups are compared to the normoxia group. Concurrent treatment with IGF-1 + LY294002 treated cultures shows greater gaps between cells compared to IGF-1 group, while concurrent treatment with Rapamycin is no different from IGF-1 alone. Each data point is the average of 3 technical replicates, and shown here is the average from 3 separate experiments. *$p < 0.05$. Bar: 100 um.

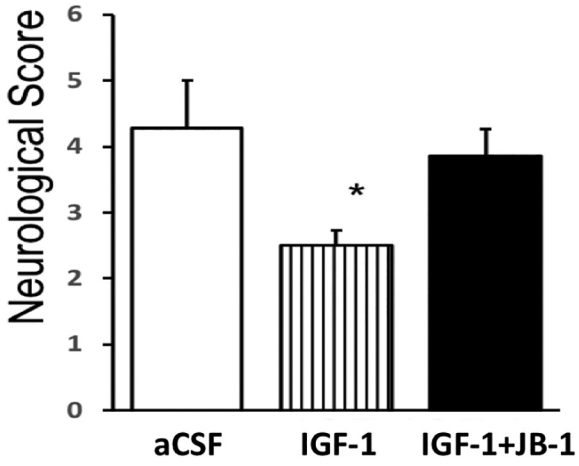

Fig. 4. Effect of post-stroke IGF-1 treatment on neurological function 1 day after MCAo. Histogram depicts mean neurological score of vehicle (artificial CSF; aCSF), IGF-1 and IGF-1 + JB-1 treated groups. Neurological function was significantly better in IGF-1-treated animals as compared to vehicle control and IGF-1 + JB-1 treated groups. All graphs represent mean ± S.E.M., n = 5–7 in each group, * $p < 0.05$.

such as MMPs that cause pathologic remodeling of the endothelium and the basement membrane. The chronic phase of stroke (days/weeks) involves regulation of apoptotic genes which leads to cell death as well as angiogenic factors that lead to repair. A recent study (Shi et al., 2016) showed that blood brain barrier leakiness seen in the earliest phase of ischemia (30 min) is independent of matrix cleavage and MMP production. During this time, BBB undergoes subtle changes including the rapid reorganization of the actin cytoskeleton in endothelial cells, which alters their morphology and permits fluid and small molecules to enter the brain, and these events precede neuronal damage. Accordingly, MMP-9 gene deletion failed to ameliorate the early leakiness of the BBB to small-sized dextrans, while overexpression of the actin depolymerization factor reduced leakiness to the small sized dextrans (Shi et al., 2016). This early 'hyper-permeability' of the BBB facilitates diapedesis of peripheral immune cells and extravasation of plasma proteins that are toxic to neurons. Our studies suggest that IGF-1 may rescue infarct volume using a similar vasculoprotective strategy. Thus, IGF-1 treatment after MCAo reduces infarct volume when measured at 24 h, which is preceded by reduced BBB hyper-permeability in the early hours after stroke (4 h) (Bake et al., 2014). The current studies build on this foundation to show that IGF-1 treatment acts directly on endothelial cells to preserve the actin cytoskeleton and its anchorage.

The in vitro model used in these studies show that the effect of IGF-1 on endothelial cell geometry is mediated by the PI3K pathway. Oxygen glucose deprivation (OGD) is commonly used to model cerebral ischemia in vitro (Doukas et al., 1994; Stanimirovic et al., 1997; Guo et al., 2012; Bake et al., 2016), and produces many of the same events seen in in vivo ischemic models, including activation of cell death pathways (Liao et al., 2016), generation of reactive oxygen species, reduced ATP production (Imai et al., 2017), and dysregulates tight junction protein expression and barrier function (Shi et al., 2016). IGF-1 is known to regulate the PI3K/Akt signaling pathway in several cell types. In mouse fibroblasts, for example, IGF-1 reduces OGD-induced cell death which is reversed by the PI3K inhibitor LY294002 (Liu et al., 2017). However, inhibition of mTOR via rapamycin did not abrogate the effect of IGF-1 on intercellular spaces. This finding is surprising since recent studies show that, in addition to its role in cell survival, autophagy, nutrient/energy sensing, mTOR is also implicated in cell adhesion (Chen et al., 2015). Alternately, this process may be mediated by mTOR2, which is rapamycin insensitive (Jacinto et al., 2004).

Changes in endothelial cell geometry is commonly seen after ischemia and ischemia-induced generation of free radicals and inflammatory cytokines (Gulino-Debrac, 2013; Stamatovic et al., 2016). Formation of thick stress fibers results in cell contractions, loss of anchorage to the matrix, and loss of tight junctions. OGD increases stress fiber formation thus changing cell geometry to a narrow, elongated form and reduces anchorage to the matrix (van der Heijden et al., 2008; Gao et al., 2012; Alluri et al., 2014). Disorganized actin cytoskeleton, such as in the dystrophin KO mouse, leads to increased vascular permeability (Nico et al., 2003), indicating the importance of actin assembly in the maintenance of the endothelial barrier. IGF-1 may alter cytoskeletal dynamics through regulation of cell adhesion via extracellular matrix proteins such as collagen and integrins(Valastyan and Weinberg, 2011). This process may occur through IGF-1 regulation of small non-coding RNA (miRNA) that act as translational repressors. Mir29 has been shown to increase collagen deposition and to improve outcomes in a renal injury model (Liu et al., 2010), and reduce fibrotic scars in a rat model of myocardial infarction (van Rooij et al., 2008). In silico analysis of vinculin shows consensus sites for mir29 and mir33, both of which are regulated by IGF-1 in vivo (Bake et al., 2016). However, further studies are warranted to examine the cytoskelelal regulatory role of these miRNAs in coordinating endothelial actin reorganization and cell-matrix adhesion under ischemia.

The present study also indicates that IGF-1 may exert different effects in the early and late acute stages of ischemia. IGF-1 has been shown to affect more immediate processes such as glucose metabolism in astrocytes (Hernandez-Garzon et al., 2016) and activation of PI-3 K/Akt signaling in microglia (Streit, 2002) and cerebellar neurons (Dudek et al., 1997), as well as long-term changes such as proliferation (Torres-Aleman et al., 1998) and neurogenesis in the hypothalamus, olfactory bulb and hippocampus (Pixley et al., 1998; Perez-Martin et al., 2010; Pardo et al., 2016). Some of these processes may be linked such that early effects on actin cytoskeleton and substrate adhesion may have durable effects on other aspects of stroke recovery such as cell survival, while others may be independent processes. This may be specifically relevant in the case of microvessel morphology. Microvessel density and diameter are reduced during occlusion of the parent vessel, and then recover gradually at reperfusion and in the days following the stroke (Dziennis et al., 2015). Thus, in the control group, the proportion of microvessels in the large bin increases from day 1 after stroke to day 5. In the IGF-1 group, the proportion of microvessels in the same large bin stays relatively stable between day 1 and day 5. Thus, it appears that IGF-1 prevents microvessel shrinkage during the crucial early period of ischemia, possibly improving microcirculation in the ischemic hemisphere, and subsequently decreasing blood brain barrier permeability and inflammation (shown in our previous studies (Bake et al., 2014; Bake et al., 2016).

In conclusion, the data from the present study underscores the importance of the microvasculature as an important early target for stroke therapies in older females, and IGF-1 as a good candidate for stroke therapy. However, defining the effective dose and timing of IGF-1 will be critical for translational applications, since the majority of stroke patients may not arrive at a medical facility prior to 2 h. While IGF-1 improves stroke recovery, its effectiveness diminishes when the treatment is delayed. In a study comparing normotensive and hypertensive male rats, subcutaneous IGF-1 significantly decreased infarct volume when given 30 mins after ischemia, but not at 2 h or 4 h later (De Geyter et al., 2013). Similarly, intranasal IGF-1 was more effective in reducing infarct volumes when given at 2 h post-stroke (54%), as compared to 4 h after stroke (39%), however behavioral improvement was only seen with early (2 h) treatment (Liu et al., 2004), similar to data from our studies. The evidence presented here shows that IGF-1's later neuroprotective actions are likely preceded by its early vasculoprotective effects.

Supplementary data to this article can be found online at https://doi.org/10.1016/j.expneurol.2018.09.016.

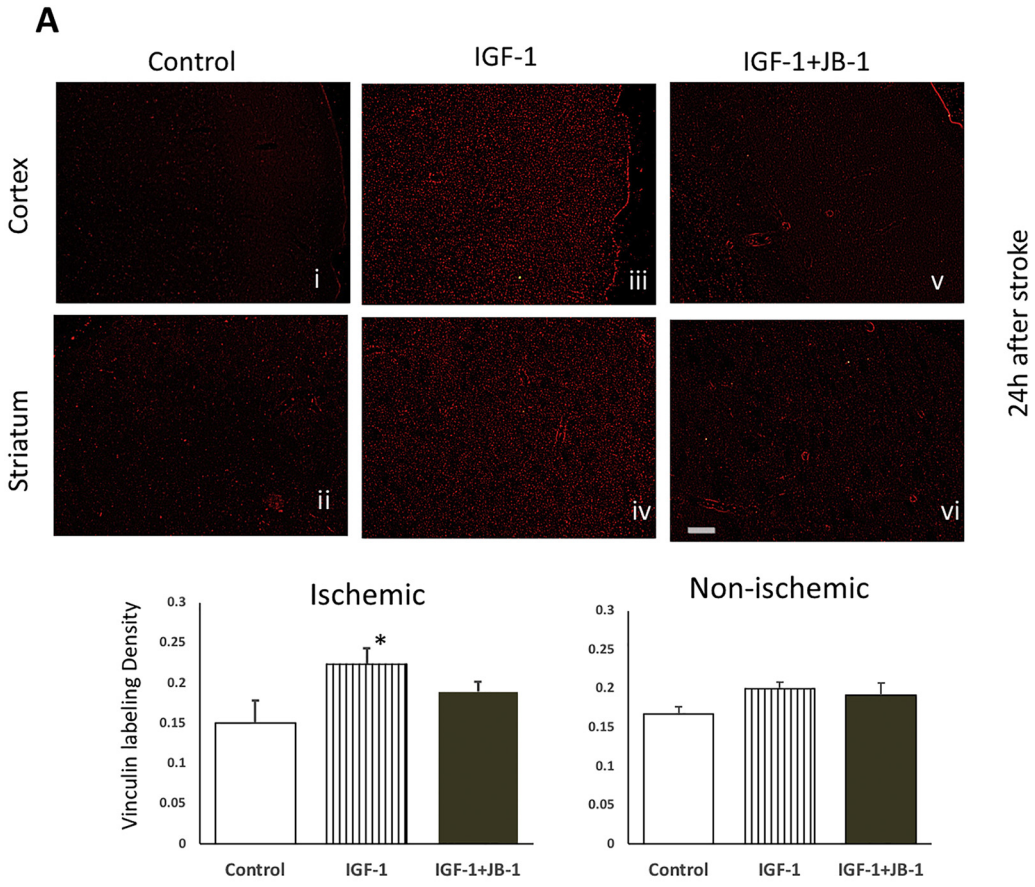

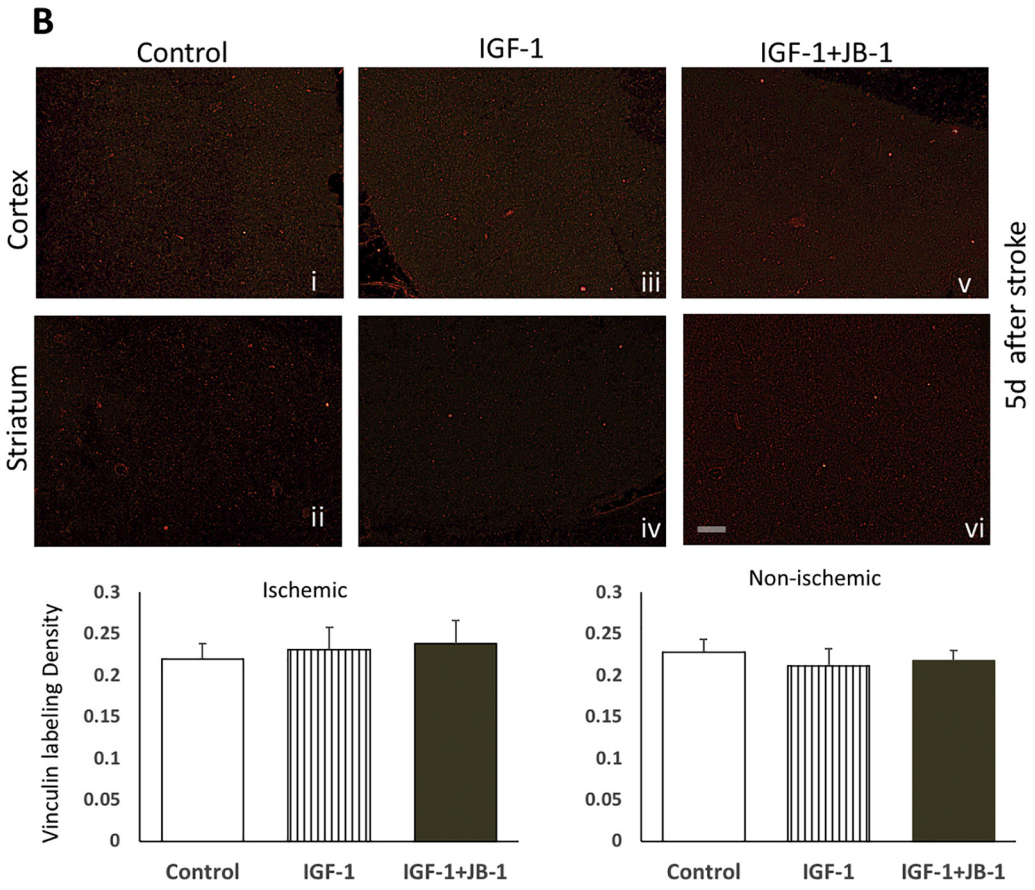

Fig. 5. Effect of post-stroke IGF-1 treatment on vinculin expression (A) 1d post stroke: Photomicrographs of vinculin immunostained representative sections from the ischemic cortex and striatum of control (i,ii), IGF-1 treated (iii,iv) and IGF-1 + JB-1 treated (v,vi) animals. Histograms depict mean and SEM of the density of vinculin staining in each group in the ischemic and non-ischemic hemisphere. (B) 5d after stroke: Photomicrographs of vinculin immunostained representative sections from the ischemic cortex and striatum of control (i,ii), IGF-1 treated (iii,iv) and IGF-1 + JB-1 treated (v,vi) animals. Histograms depict mean and SEM of the density of vinculin staining in each group in the ischemic and non-ischemic hemisphere. N = 4–6 in each group. *: $p < 0.05$. Bar: 100 um.

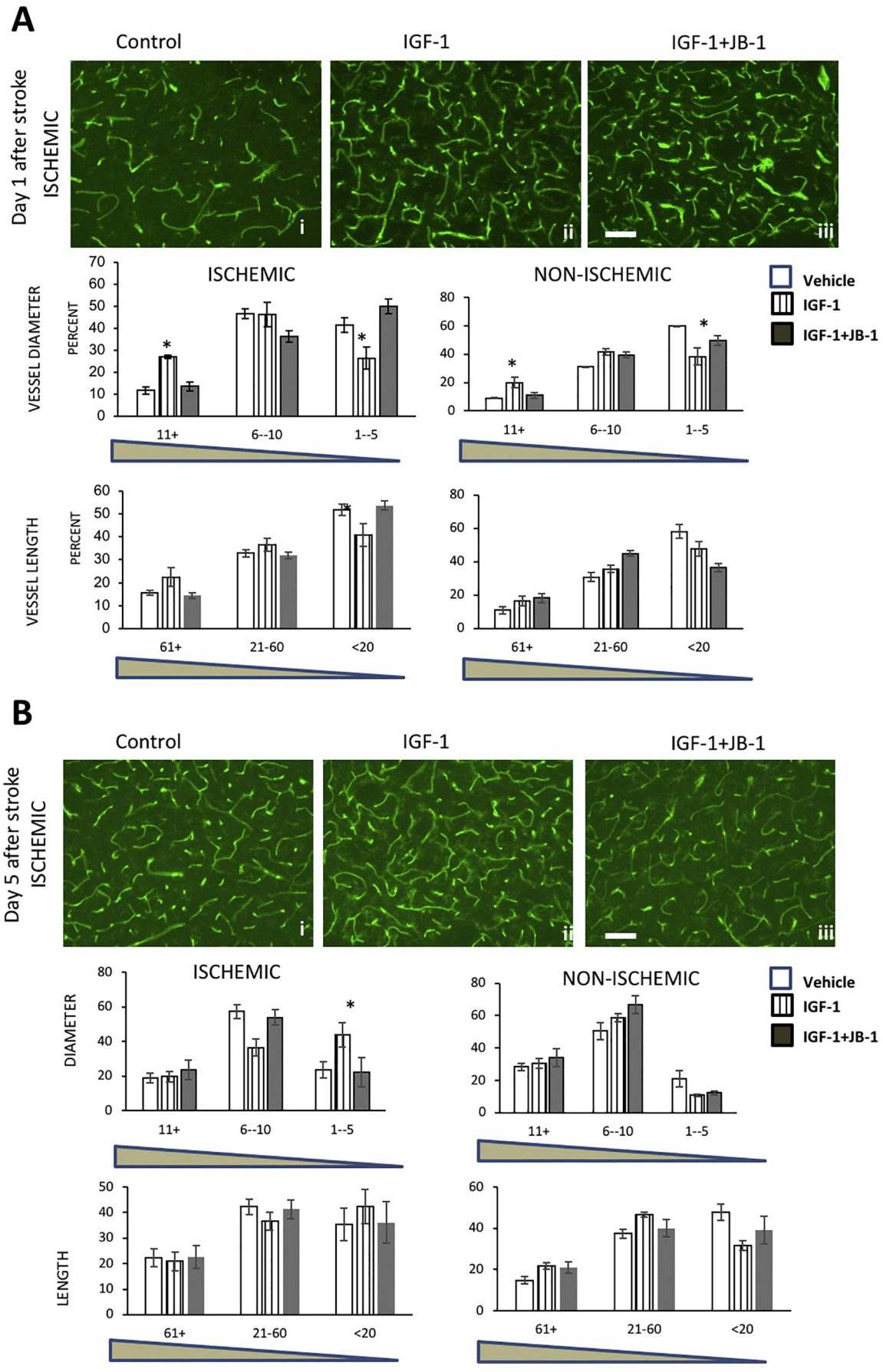

(caption on next page)

Fig. 6. Effect of post-stroke IGF-1 treatment on microvessel morphology. (A) 1d post stroke: Photomicrographs of lectin-sectioned microvessels from the ischemic hemisphere of control (i), IGF-1 treated (ii) and IGF-1 + JB-1 treated (iii) animals. Histograms depict the mean distribution of microvessel diameter (top) and microvessel length (bottom) from the ischemic and non-ischemic hemisphere. IGF-1 treated animals showed greater number of vessels in the largest bin (11 +) compared to vehicle control or IGF + JB-1 treated groups in both ischemic and non-ischemic sides, and fewer short length vessels on the ischemic hemisphere. * $p < 0.05$, main effect of IGF1 treatment. (B) 5d post stroke: Photomicrographs of lectin-stained microvessels from the ischemic hemisphere of control (i), IGF-1 treated (ii) and IGF-1 + JB-1 treated (iii) animals. Histograms depict the mean distribution of microvessel diameter (top) and microvessel length (bottom) from the ischemic and non-ischemic hemisphere. IGF-1-treated animals showed greater number of small diameter vessels as compared to other two groups in the ischemic hemisphere. N = 4–6 in each group. * $p < 0.05$, Bar: 100 um.

Acknowledgements

Supported by NS074895 from the NIH and a Discovery Foundation grant to FS. The authors are grateful to Ms. Tiffany Heard, Mr. Victor Cardenas and Ms. Jessica Lee for their technical assistance.

References

Alluri, H., Stagg, H.W., Wilson, R.L., Clayton, R.P., Sawant, D.A., Koneru, M., Beeram, M.R., Davis, M.L., Tharakan, B., 2014. Reactive oxygen species-caspase-3 relationship in mediating blood-brain barrier endothelial cell hyperpermeability following oxygen-glucose deprivation and reoxygenation. Microcirculation 21, 187–195.

Bake, S., Selvamani, A., Cherry, J., Sohrabji, F., 2014. Blood brain barrier and neuroinflammation are critical targets of IGF-1-mediated neuroprotection in stroke for middle-aged female rats. PLoS One 9, e91427.

Bake, S., Okoreeh, A.K., Alaniz, R.C., Sohrabji, F., 2016. Insulin-like growth factor (IGF)-I modulates endothelial blood-brain barrier function in ischemic middle-aged female rats. Endocrinology 157, 61–69.

Baldo, C., Lopes, D.S., Faquim-Mauro, E.L., Jacysyn, J.F., Niland, S., Eble, J.A., Clissa, P.B., Moura-Da-Silva, A.M., 2015. Jararhagin disruption of endothelial cell anchorage is enhanced in collagen enriched matrices. Toxicon 108, 240–248.

Borlongan, C.V., Glover, L.E., Sanberg, P.R., Hess, D.C., 2012. Permeating the blood brain barrier and abrogating the inflammation in stroke: implications for stroke therapy. Curr. Pharm. Des. 18, 3670–3676.

Chen, L., Xu, B., Liu, L., Liu, C., Luo, Y., Chen, X., Barzegar, M., Chung, J., Huang, S., 2015. Both mTORC1 and mTORC2 are involved in the regulation of cell adhesion. Oncotarget 6, 7136–7150.

De Geyter, D., Stoop, W., Sarre, S., De Keyser, J., Kooijman, R., 2013. Neuroprotective efficacy of subcutaneous insulin-like growth factor-I administration in normotensive and hypertensive rats with an ischemic stroke. Neuroscience 250, 253–262.

Dimitrijevic, O.B., Stamatovic, S.M., Keep, R.F., Andjelkovic, A.V., 2007. Absence of the chemokine receptor CCR2 protects against cerebral ischemia/reperfusion injury in mice. Stroke 38, 1345–1353.

Dinapoli, V.A., Huber, J.D., Houser, K., Li, X., Rosen, C.L., 2008. Early disruptions of the blood-brain barrier may contribute to exacerbated neuronal damage and prolonged functional recovery following stroke in aged rats. Neurobiol. Aging 29, 753–764.

Doukas, J., Cutler, A.H., Boswell, C.A., Joris, I., Maino, G., 1994. Reversible endothelial cell relaxation induced by oxygen and glucose deprivation. A model of ischemia in vitro. Am. J. Pathol. 145, 211–219.

Dudek, H., Datta, S.R., Franke, T.F., Birnbaum, M.J., Yao, R., Cooper, G.M., Segal, R.A., Kaplan, D.R., Greenberg, M.E., 1997. Regulation of neuronal survival by the serine-threonine protein kinase Akt. Science 275, 661–665.

Dziennis, S., Qin, J., Shi, L., Wang, R.K., 2015. Macro-to-micro cortical vascular imaging underlies regional differences in ischemic brain. Sci. Rep. 5, 10051.

Gao, C., Li, R., Liu, Y., Ma, L., Wang, S., 2012. Rho-kinase-dependent F-actin rearrangement is involved in the release of endothelial microparticles during IFN-alpha-induced endothelial cell apoptosis. J. Trauma Acute Care Surg. 73, 1152–1160.

Gidday, J.M., Gasche, Y.G., Copin, J.C., Shah, A.R., Perez, R.S., Shapiro, S.D., Chan, P.H., Park, T.S., 2005. Leukocyte-derived matrix metalloproteinase-9 mediates blood-brain barrier breakdown and is proinflammatory after transient focal cerebral ischemia. Am. J. Physiol. Heart Circ. Physiol. 289, H558–H568.

Gluckman, P., Klempt, N., Guan, J., Mallard, C., Sirimanne, E., Dragunow, M., Klempt, M., Singh, K., Williams, C., Nikolics, K., 1992. A role for IGF-1 in the rescue of CNS neurons following hypoxic-ischemic injury. Biochem. Biophys. Res. Commun. 182, 593–599.

Guan, J., Miller, O.T., Waugh, K.M., McCarthy, D.C., Gluckman, P.D., 2001. Insulin-like growth factor-1 improves somatosensory function and reduces the extent of cortical infarction and ongoing neuronal loss after hypoxia-ischemia in rats. Neuroscience 105, 299–306.

Gulino-Debrac, D., 2013. Mechanotransduction at the basis of endothelial barrier function. Tissue Barriers 1, e24180.

Guo, J., Duckles, S.P., Weiss, J.H., Li, X., Krause, D.N., 2012. 17beta-Estradiol prevents cell death and mitochondrial dysfunction by an estrogen receptor-dependent mechanism in astrocytes after oxygen-glucose deprivation/reperfusion. Free Radic. Biol. Med. 52, 2151–2160.

Hernandez-Garzon, E., Fernandez, A.M., Perez-Alvarez, A., Genis, L., Bascunana, P., Fernandez De La Rosa, R., Delgado, M., Angel Pozo, M., Moreno, E., McCormick, P.J., Santi, A., Trueba-Saiz, A., Garcia-Caceres, C., Tschop, M.H., Araque, A., Martin, E.D., Torres Aleman, I., 2016. The insulin-like growth factor I receptor regulates glucose transport by astrocytes. Glia 64, 1962–1971.

Imai, T., Mishiro, K., Takagi, T., Isono, A., Nagasawa, H., Tsuruma, K., Shimazawa, M., Hara, H., 2017. Protective effect of bendavia (SS-31) against oxygen/glucose-deprivation stress-induced mitochondrial damage in human brain microvascular endothelial cells. Curr. Neurovasc. Res. 14, 53–59.

Jacinto, E., Loewith, R., Schmidt, A., Lin, S., Ruegg, M.A., Hall, A., Hall, M.N., 2004. Mammalian TOR complex 2 controls the actin cytoskeleton and is rapamycin insensitive. Nat. Cell Biol. 6, 1122–1128.

Johnston, B.M., Mallard, E.C., Williams, C.E., Gluckman, P.D., 1996. Insulin-like growth factor-1 is a potent neuronal rescue agent after hypoxic-ischemic injury in fetal lambs. J. Clin. Invest. 97, 300–308.

Khatri, R., McKinney, A.M., Swenson, B., Janardhan, V., 2012. Blood-brain barrier, reperfusion injury, and hemorrhagic transformation in acute ischemic stroke. Neurology 79, S52–S57.

Kleinschnitz, C., Wiendl, H., 2013. Con: Regulatory T cells are protective in ischemic stroke. Stroke 44, e87–e88.

Kreuger, J., Phillipson, M., 2016. Targeting vascular and leukocyte communication in angiogenesis, inflammation and fibrosis. Nat. Rev. Drug Discov. 15, 125–142.

Lee, W.H., Clemens, J.A., Bondy, C.A., 1992. Insulin-like growth factors in the response to cerebral ischemia. Mol. Cell. Neurosci. 3, 36–43.

Liao, L.X., Zhao, M.B., Dong, X., Jiang, Y., Zeng, K.W., Tu, P.F., 2016. TDB protects vascular endothelial cells against oxygen-glucose deprivation/reperfusion-induced injury by targeting miR-34a to increase Bcl-2 expression. Sci. Rep. 6, 37959.

Liu, X.F., Fawcett, J.R., Hanson, L.R., Frey 2nd, W.H., 2004. The window of opportunity for treatment of focal cerebral ischemic damage with noninvasive intranasal insulin-like growth factor-I in rats. J. Stroke Cerebrovasc. Dis. 13, 16–23.

Liu, F., Yuan, R., Benashski, S.E., McCullough, L.D., 2009. Changes in experimental stroke outcome across the life span. J. Cereb. Blood Flow Metab. 29, 792–802.

Liu, Y., Taylor, N.E., Lu, L., Usa, K., Cowley Jr., A.W., Ferreri, N.R., Yeo, N.C., Liang, M., 2010. Renal medullary microRNAs in Dahl salt-sensitive rats: miR-29b regulates several collagens and related genes. Hypertension 55, 974–982.

Liu, Q., Guan, J.Z., Sun, Y., Le, Z., Zhang, P., Yu, D., Liu, Y., 2017. Insulin-like growth factor 1 receptor-mediated cell survival in hypoxia depends on the promotion of autophagy via suppression of the PI3K/Akt/mTOR signaling pathway. Mol. Med. Rep. 15, 2136–2142.

Merali, S., Cameron, J.I., Barclay, R., Salbach, N.M., 2016. Characterising community exercise programmes delivered by fitness instructors for people with neurological conditions: a scoping review. Health Soc. Care Community 24, e101–e116.

Montagne, A., Barnes, S.R., Sweeney, M.D., Halliday, M.R., Sagare, A.P., Zhao, Z., Toga, A.W., Jacobs, R.E., Liu, C.Y., Amezcua, L., Harrington, M.G., Chui, H.C., Law, M., Zlokovic, B.V., 2015. Blood-brain barrier breakdown in the aging human hippocampus. Neuron 85, 296–302.

Moskowitz, M.A., Lo, E.H., Iadecola, C., 2010. The science of stroke: mechanisms in search of treatments. Neuron 67, 181–198.

Nico, B., Frigeri, A., Nicchia, G.P., Corsi, P., Ribatti, D., Quondamatteo, F., Herken, R., Girolamo, F., Marzullo, A., Svelto, M., Roncali, L., 2003. Severe alterations of endothelial and glial cells in the blood-brain barrier of dystrophic mdx mice. Glia 42, 235–251.

Okoreeh, A.K., Bake, S., Sohrabji, F., 2017. Astrocyte-specific insulin-like growth factor-1 gene transfer in aging female rats improves stroke outcomes. Glia 65, 1043–1058.

Pardo, J., Uriarte, M., Console, G.M., Reggiani, P.C., Outeiro, T.F., Morel, G.R., Goya, R.G., 2016. Insulin-like growth factor-I gene therapy increases hippocampal neurogenesis, astrocyte branching and improves spatial memory in female aging rats. Eur. J. Neurosci. 44, 2120–2128.

Paxinos, G., Watson, C., 1986. The Rat Brain in Stereotaxic Coordinates. Academic Press Inc, New York.

Perez-Martin, M., Cifuentes, M., Grondona, J.M., Lopez-Avalos, M.D., Gomez-Pinedo, U., Garcia-Verdugo, J.M., Fernandez-Llebrez, P., 2010. IGF-I stimulates neurogenesis in the hypothalamus of adult rats. Eur. J. Neurosci. 31, 1533–1548.

Pixley, S.K., Dangoria, N.S., Odoms, K.K., Hastings, L., 1998. Effects of insulin-like growth factor 1 on olfactory neurogenesis in vivo and in vitro. Ann. N. Y. Acad. Sci. 855, 244–247.

Pulsinelli, W., 1992. Pathophysiology of acute ischaemic stroke. Lancet 339, 533–536.

Selvamani, A., Sohrabji, F., 2010a. The neurotoxic effects of estrogen on ischemic stroke in older female rats is associated with age-dependent loss of insulin-like growth factor-1. J. Neurosci. 30, 6852–6861.

Selvamani, A., Sohrabji, F., 2010b. Reproductive age modulates the impact of focal ischemia on the forebrain as well as the effects of estrogen treatment in female rats. Neurobiol. Aging 31, 1618–1628.

Shen, Q., Wu, M.H., Yuan, S.Y., 2009. Endothelial contractile cytoskeleton and microvascular permeability. Cell Health Cytoskeleton 2009, 43–50.

Shi, Y., Zhang, L., Pu, H., Mao, L., Hu, X., Jiang, X., Xu, N., Stetler, R.A., Zhang, F., Liu, X., Leak, R.K., Keep, R.F., Ji, X., Chen, J., 2016. Rapid endothelial cytoskeletal reorganization enables early blood-brain barrier disruption and long-term ischaemic reperfusion brain injury. Nat. Commun. 7, 10523.

Smith, P.F., 2003. Neuroprotection against hypoxia-ischemia by insulin-like growth

factor-I (IGF-I). IDrugs 6, 1173–1177.
Stamatovic, S.M., Johnson, A.M., Keep, R.F., Andjelkovic, A.V., 2016. Junctional proteins of the blood-brain barrier: New insights into function and dysfunction. Tissue Barriers 4, e1154641.
Stanimirovic, D.B., Ball, R., Durkin, J.P., 1997. Stimulation of glutamate uptake and Na,K-ATPase activity in rat astrocytes exposed to ischemia-like insults. Glia 19, 123–134.
Streit, W.J., 2002. Microglia as neuroprotective, immunocompetent cells of the CNS. Glia 40, 133–139.
Torres-Aleman, I., Villalba, M., Nieto-Bona, M.P., 1998. Insulin-like growth factor-I modulation of cerebellar cell populations is developmentally stage-dependent and mediated by specific intracellular pathways. Neuroscience 83, 321–334.
Valastyan, S., Weinberg, R.A., 2011. Roles for microRNAs in the regulation of cell adhesion molecules. J. Cell Sci. 124, 999–1006.
van der Heijden, M., Versteilen, A.M., Sipkema, P., van Nieuw Amerongen, G.P., Musters, R.J., Groeneveld, A.B., 2008. Rho-kinase-dependent F-actin rearrangement is involved in the inhibition of PI3-kinase/Akt during ischemia-reperfusion-induced endothelial cell apoptosis. Apoptosis 13, 404–412.
van Rooij, E., Sutherland, L.B., Thatcher, J.E., Dimaio, J.M., Naseem, R.H., Marshall, W.S., Hill, J.A., Olson, E.N., 2008. Dysregulation of microRNAs after myocardial infarction reveals a role of miR-29 in cardiac fibrosis. Proc. Natl. Acad. Sci. U. S. A. 105, 13027–13032.
Wang, J.M., Hayashi, T., Zhang, W.R., Sakai, K., Shiro, Y., Abe, K., 2000. Reduction of ischemic brain injury by topical application of insulin-like growth factor-I after transient middle cerebral artery occlusion in rats. Brain Res. 859, 381–385.
Wu, L., Walas, S., Leung, W., Sykes, D.B., Wu, J., Lo, E.H., Lok, J., 2015. Neuregulin1-beta decreases IL-1beta-induced neutrophil adhesion to human brain microvascular endothelial cells. Transl Stroke Res 6, 116–124.
Yang, Y., Estrada, E.Y., Thompson, J.F., Liu, W., Rosenberg, G.A., 2007. Matrix metalloproteinase-mediated disruption of tight junction proteins in cerebral vessels is reversed by synthetic matrix metalloproteinase inhibitor in focal ischemia in rat. J. Cereb. Blood Flow Metab. 27, 697–709.
Zhu, L., Han, B., Wang, L., Chang, Y., Ren, W., Gu, Y., Yan, M., Wu, C., Zhang, X.Y., He, J., 2016. The association between serum ferritin levels and post-stroke depression. J. Affect. Disord. 190, 98–102.